Morphological Control of Nanocrystalline Aluminum Nitride: Aluminum Chloride-Assisted Nanowhisker Growth
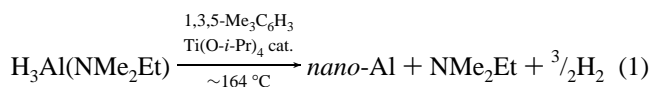
Joel A. Haber,[†] Patrick C. Gibbons,[‡] and William E. Buhro*,[†]

Departments of Chemistry and Physics
Washington University
St. Louis, Missouri, 63130-4899

Received September 25, 1996

Herein we report a morphologically selective synthesis of nanocrystalline aluminum nitride (*nano*-AlN) by low-temperature nitridation of nanocrystalline aluminum (*nano*-Al).[1] Particle morphologies are varied from predominantly equiaxed to predominantly whisker-like, apparently by the presence of vapor-transport species during nitridation. Whisker formation appears to be due to an increased volatility of aluminum induced by the large surface area of *nano*-Al and the action of volatile aluminum chlorides. The altered electronic, magnetic, and mechanical properties of nanocrystalline materials have received much emphasis;[2] our results illustrate their altered reactivities.[3] To our knowledge, procedures allowing selective synthesis of various nanoparticle morphologies by purposeful variations in reaction conditions are rare.[4]

Air-sensitive *nano*-Al was produced by the catalytic decomposition of $H_3Al(NMe_2Et)$[5] with $Ti(O\text{-}i\text{-}Pr)_4$ (0.05−1.2 mol %, eq 1). The *nano*-Al powders were 99 wt % Al by elemental

$$H_3Al(NMe_2Et) \xrightarrow[\sim 164\,°C]{\substack{1,3,5\text{-Me}_3C_6H_3 \\ Ti(O\text{-}i\text{-}Pr)_4 \text{ cat.}}} nano\text{-}Al + NMe_2Et + {}^3\!/_2 H_2 \quad (1)$$

analysis,[6] and mean crystallite dimensions of 40−180 nm were determined by Scherrer analysis of XRD line broadening.[7]

† Department of Chemistry.
‡ Department of Physics.
(1) For other syntheses of *nano*-AlN, see: (a) Vissokov, G. P.; Stefanov, B. I.; Gerasimov, N. T.; Oliver, D. H.; Enikov, R. Z.; Vrantchev, A. I.; Balabanova, E. G.; Pirgov, P. S. *J. Mater. Sci.* **1988**, *23*, 2415−2418. (b) Chow, G. M.; Xiao, T. D.; Chen, X.; Gonsalves, K. E. *J. Mater. Res.* **1994**, *9*, 168−174. (c) Wade, T.; Park, J.; Garza, E. G.; Ross, C. B.; Smith, D. M.; Crooks, R. M. *J. Am. Chem. Soc.* **1992**, *114*, 9457−9464. (d) Bolt, J. D.; Tebbe, F. N. In *Advances in Ceramics*; American Ceramic Society: Westerville, OH, 1989; Vol 26, pp 69−76. (e) Ramesh, P. D.; Rao, K. J. *Adv. Mater.* **1995**, *7*, 177−17. (f) Adjaottor, A. A.; Griffin, G. L. *J. Am. Ceram. Soc.* **1992**, *75*, 3209−3214. (g) Jung, W.-S.; Ahn, S.-K. *J. Mater. Chem.* **1994**, *4*, 949−953. (h) Johnston, G. P.; Muenchausen, R. E.; Smith, D. M.; Foltyn, S. R. *J. Am. Ceram. Soc.* **1992**, *75*, 3465−3468. (i) Sood, R. R.; Southam, F. W.; Raghavan, N. S. Eur. Pat. 88308209.1, 1989, document number 0 308 116 A1, *Chem. Abstr.* an 111:9752 ca. (j) Pratsinis, S. E.; Wang, G.; Panda, S.; Guiton, T. Weimer, A. W. *J. Mater. Res.* **1995**, *10*, 512−520.
(2) (a) Andres, R. P.; Averback, R. S.; Brown, W. L.; Brus, L. E.; Goddard, W. A., III; Kaldor, A.; Louie, S. G.; Moscovits, M.; Peercy, P. S.; Riley, S. J.; Siegel, R. W.; Spaepen, F.; Wang, Y. *J. Mater. Res.* **1989**, *4*, 704−736. (b) Gleiter, H. *Prog. Mater. Sci.* **1989**, *33*, 223−315.
(3) Rieke, R. D. *Science* **1989**, *246*, 1260−1264.
(4) (a) Ahmadi, T. S.; Wang, Z. L.; Green, T. C.; Henglein, A.; El-Sayed, M. A. *Science* **1996**, *272*, 1924−1926. (b) Tanori, J.; Pileni, M. P. *Adv. Mater.* **1995**, *7*, 862−864.
(5) Frigo, D. M.; van Eijden, G. J. M.; Reuvers, P. J.; Smit, C. J. *Chem. Mater.* **1994**, *6*, 190−195. A powerful explosion occurred during the synthesis of $H_3Al(NMe_2Et)$, which extensively deformed a steel fume-hood enclosure. Details are in the Supporting Information.
(6) *nano*-Al (28 nm) produced using 0.5 mol % $Ti(O\text{-}i\text{-}Pr)_4$ was consolidated by hot pressing at 100 °C for 1 h at 350 MPa in an Ar-filled glove box. Elemental analysis of a portion of this pellet was performed by Glow Discharge Mass Spectrometry analyzing for 25 elements. The primary impurities were (wt %): C, 0.23; O, 0.25; N, 0.055; Cl, 0.14; Ti, 0.32; Al, 99.0 (by difference). Minor impurities were (ppm by wt): Li, 1.3; B, 0.15; F, <0.05; Na, 2.9; Mg, 0.37; Si, 40; S, 1.8; K, 4.8; Ca, 0.61; Cr, 0.5; Mn, 0.01; Fe, 1.5; Ni, 0.35; Cu, 0.4; Zn, 0.27; Ga, 0.12; Mo, 0.9; In, 1.9; Ta, <1; W, 0.05.
(7) The coherence length of Al produced by decomposition of H_3Al-(NMe_2Et) changes as a function of mol % $Ti(O\text{-}i\text{-}Pr)_4$.

Transmission electron microscopy (TEM) revealed 0.5−5 μm aggregates of 10−200 nm Al crystallites (Figure 1a).

Reaction of the *nano*-Al with N_2 at 1000−1100 °C resulted in complete conversion to *nano*-AlN (25−50 nm mean coherence length by XRD).[8] The morphology of the *nano*-AlN was almost entirely equiaxed (Figure 1b) when pure *nano*-Al or when *nano*-Al mixed with an inert additive was heated at 20 °C/min to 1000 or 1100 °C. The morphological distribution of the *nano*-AlN was altered to favor the formation of nanowhiskers by addition of $AlCl_3$ to the *nano*-Al before heating or by increasing the heating rate. Addition of $AlCl_3$ also improved the purity of the AlN produced.[9] Increasing the amount of $AlCl_3$ added and increasing the heating rate produced larger fractions of nanowhiskers (up to *ca.* 90%, Figure 1c).

Nanocrystalline AlN was also obtained by nitridation of commercial 2 and 20 μm Al[10] under identical conditions. The changes in the morphological distribution of the *nano*-AlN produced from the commercial powders mirrored the changes observed with *nano*-Al, but lower fractions of nanowhiskers were obtained, and the nitridation did not go to completion.[11] Microscopy of partially reacted samples revealed a significant fraction of nanowhiskers in all cases and that addition of $AlCl_3$ increased the whisker fraction.

The whiskers were single crystalline as shown by selected area diffraction (SAD) and were generally 20−100 nm in diameter with aspect ratios (length/diameter) of 20 to >100. When 10 wt % of $AlCl_3$ was added and a heating rate of 20 °C/min was used, most of the whiskers were straight, but unusual growth morphologies were also observed such as bent, curved, axe-shaped, hexagonal cone, and a hollow tube. When 93 wt % of $AlCl_3$ was added and/or when a heating rate of >50 °C/min was used branched and comblike crystals were common, indicating a significant change in growth kinetics that made additional growth directions accessible.

Among the known whisker-growth mechanisms, the vapor−liquid−solid (VLS) and vapor−solid (VS) mechanisms are the most likely to function under the present conditions.[12] In the VLS mechanism, whiskers grow from liquid flux droplets attached to whisker tips. We observed no such flux droplets, and addition of various potential flux materials did not promote whisker formation.[12] Additionally, the variety of observed crystallite morphologies and whisker-growth directions is more

(8) In a typical run, the MgO tube was loaded with *nano*-Al, 2 μm Al, 20 μm Al, or an Al/$AlCl_3$ mixture and inserted into a fused-silica tube sealed on one end and fitted with an Ultratorr valve assembly on the other end. The assembly was removed from the glovebox, and the MgO tube was placed into a tube furnace. After appropriate purging of the connecting lines, the valve was opened to N_2 (1 atm). The sample was heated to 900−1100 °C for 15 min to 10 h to produce *nano*-AlN.
(9) *nano*-AlN was prepared by heating *nano*-Al under N_2 at 1100 °C for 10 h. Elemental analysis performed by Galbraith laboratories with airless handling found (wt %): Al, 63.5; N, 32.2; Ti, 0.32; C, <0.5; Mg, <0.06; O, <4.6 (by difference). *nano*-AlN was also prepared by mixing *nano*-Al with 9.3 wt % $AlCl_3$ and treating it identically to the previous sample. Anal. found (wt %): Al, 66.4; N, 31.9; Cl, 0.27; Ti, <0.09; C, 0.56; Mg, <0.09; O, <0.9 (by difference). Calcd (wt %): Al, 65.8; N, 34.2.
(10) The 2 μm Al (Strem) ranged from 0.5 to 20 μm in diameter, and the 20 μm powder (Aldrich) ranged from 2 to 75 μm in diameter, as determined by SEM.
(11) Aluminum powder (2−3 μm mean particle size) was reacted with N_2 at 1100 °C as received and with 13 wt % added $AlCl_3$. XRD patterns of both products showed peaks for *nano*-AlN only; however, TEM showed that both products contained spherical aggregates (≥200 nm diameter) of equiaxed particles (≤20 nm diameter) with excess Al by energy-dispersive X-ray spectroscopy. Significantly, the Al without $AlCl_3$ produced very few whiskers, whereas the Al with added $AlCl_3$ produced a large yield of nanowhiskers. We believe that the 2−3 μm Al powder is at the crossover point between *nano*-Al, which nitrides completely, and coarse Al powder, which does not nitride completely under these conditions.
(12) (a) Givargizov, E. I. In *Current Topics in Materials Science*; Kaldis, E., Ed; North-Holland Publishing: New York, 1978; Vol. 1, p 22. (b) Givargizov, E. E. *J. Cryst. Growth* **1975**, *31*, 20−30. (c) Campbell, W. B. In *Whisker Technology*; Levitt, A. P., Ed.; Wiley-Interscience: New York, 1970; pp 17, 27, and 28.
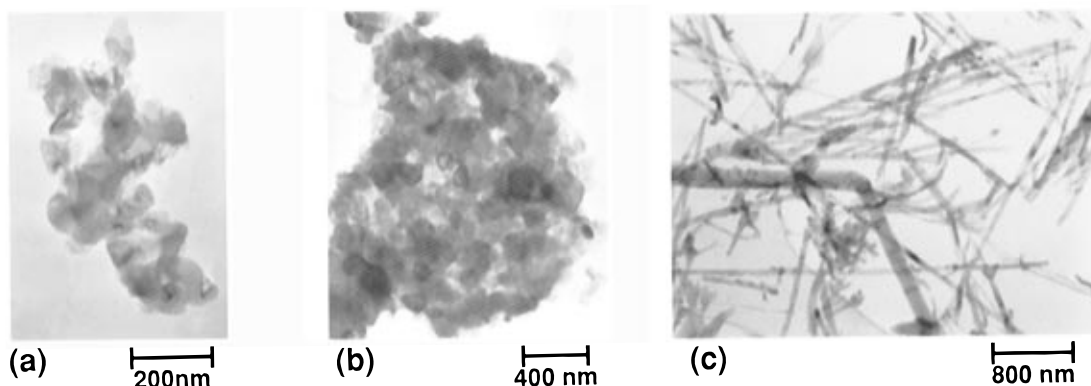
Figure 1. TEM micrographs of *nano*-Al from eq 1 (a) and the two principal *nano*-AlN morphologies produced from it: *nano*-AlN equiaxed crystallites (b), and AlN nanowhiskers and a highly branched crystallite produced by adding 93 wt % AlCl$_3$ and using a heating rate of 100 °C/min (c).

consistent with VS growth than with VLS growth.[12]

VS growth is apparently supported by the large *nano*-Al surface area, which increases the effective steady-state Al vapor pressure. The *equilibrium* Al vapor pressure predicted by the Kelvin equation[13] is increased by at most 2−3% for the *nano*-Al (44 nm mean coherence length) used. However, the system is not in equilibrium because the Al vapor is reacting to form AlN. The increased rate of evaporation afforded by the large surface area of *nano*-Al likely produces a larger *steady-state* vapor pressure than is present over coarser Al particles. The increased Al vapor pressure enables growth of a small number of whiskers even when AlCl$_3$ is not added. However, in the absence of AlCl$_3$, we observe that the whisker fraction decreases significantly as the Al particles sinter and melt into larger droplets, which become coated with AlN.

The dramatic increase in whisker fraction upon addition of AlCl$_3$ supports a mechanism in which AlCl$_3$ acts as a transport agent. AlCl$_3$ did not maintain Al particle sizes at nanometer dimensions; partially reacted Al/AlN droplets ranged from 5−15 μm *with* or *without* added AlCl$_3$, and nitridation of 2 or 20 μm Al with AlCl$_3$ added produced a large whisker fraction. However, AlCl$_3$ changed the morphology of the partially reacted droplets. When no AlCl$_3$ was added, all of the partially reacted Al formed spherical balls covered with a stubble of AlN particles.[14] When 10 wt % of AlCl$_3$ was added, about half of the partially reacted Al formed spherical balls covered with long fibers or whiskers and half of the Al formed starfish-like particles which were partially nitrided, but had smooth surfaces. In completely reacted samples to which 10 wt % AlCl$_3$ had been added, some of the AlN shells had holes revealing a hollowed interior, indicating that Al was removed from the core during the reaction. AlCl$_3$ was likely thus a transport agent for Al removal from partially nitrided droplets.

AlCl$_3$(g) and Al(l) are known to form significant equilibrium quantities of AlCl(g) at the nitridation temperatures employed.[15] Therefore, it is likely that AlCl participates in the formation of AlN whiskers as proposed in Figure 2. The mixture of *nano*-Al and AlCl$_3$ produced a greater fraction of whiskers than did the mixture of 2 or 20 μm Al and AlCl$_3$ because the *nano*-Al affords a much larger surface area, which increases the rate of the interfacial reaction between Al(l) and AlCl$_3$.
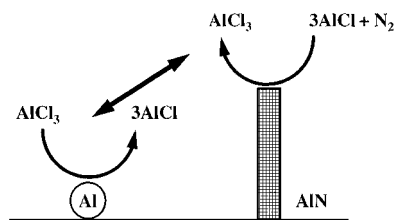

Figure 2. Proposed vapor-transport process for whisker growth.

Rapid heating rates and small Al particle sizes increase the whisker fraction by maximizing the surface area and the AlCl$_3$ concentration when the nitridation temperature is reached. The reaction between Al(l) and N$_2$ to form AlN begins at *ca.* 1073 K, 140 K above the melting point of Al.[7] A faster heating rate reduces the time during which Al particles may coalesce before nitridation begins, resulting in smaller droplet sizes. Once nitridation begins further droplet growth is prevented by formation of a shell of AlN particles. A faster heating rate also decreases the amount of AlCl$_3$ that sublimes out of the system before nitridation begins, effectively increasing the concentration of AlCl$_3$ in the reacting system.

Thus, the enhanced reactivity of *nano*-Al allows the low-temperature synthesis of AlN with morphological control. Direct surface nitridation of *coarse*-grained Al results in an AlN surface coating that inhibits complete nitridation at the temperatures we employed.[11,16] In contrast, the small particles in *nano*-Al are completely nitrided. Additionally, the high surface area of *nano*-Al amplifies the proposed AlCl$_3$/AlCl VS whisker-growth mechanism, producing large yields of AlN nanowhiskers that are among the smallest known.[17]

(13) (a) Atkins, P. W. *Physical Chemistry*, 4th ed.; W. H. Freeman: New York, 1990; p 158. (b) The equilibrium vapor pressure can also be calculated using the Gibbs−Thompson equation.[20c] (c) Jena, A. K.; Chaturvedi, M. C. *Phase Transformations in Materials*; Prentice-Hall: Englewood Cliffs, NJ, 1992; p 59.

(14) The "stubble" coating the partially reacted Al droplets appears to be fibrous aggregates of equiaxed particles. It is not possible to distinguish single-crystal whiskers from dense polycrystalline fibers by SEM; however, the bent, conelike appearance of much of the "stubble" and "hair" on the Al droplets suggests that they are not whiskers, but rather polycrystalline. Fragments of similarly shaped structures are seen to be polycrystalline by TEM.

(15) Roa, D. B.; Dadape, V. V. *J. Phys. Chem.* **1966**, *70*, 1349−1353.

(16) Weimer, A. W.; Cochran, G. A.; Eisman, G. A.; Henley, J. P.; Hook, B. D.; Mills, L. K.; Guiton, T. A.; Knudsen, A. K.; Nicholas, N. R.; Volmering, J. E.; Moore, W. G. *J. Am. Ceram. Soc.* **1994**, *77*, 3−18.

(17) (a) Tadashi, Y.; Katsutoshi, N.; Akihisa, I.; Tsuyoshi, M. Eur. Pat. 94114147.5, 1994. (b) Yamaguchi, T.; Inoue, A.; Nosaki, K.; Nakane, H. *Mater. Trans. JIM* **1994**, *35*, 538−542.